

Producing Multiple Qubits via Spontaneous Parametric Down-Conversion

Phillip Heitert,[†] Finn Buldt^{‡,†}, Pascal Bassène, and Moussa N’Gom^{‡,*}

Department of Physics, Rensselaer Polytechnic Institute, 110 8th Street, Troy, New York 12180, USA



(Received 11 May 2021; revised 19 August 2021; accepted 15 November 2021; published 20 December 2021)

We present a simple approach to produce multiple correlated photon pairs through spontaneous parametric down-conversion. We develop Gaussian masks to subdivide the pump beam before passing it through a nonlinear medium. In this way, we are able to observe simultaneous separate down-converted emission cones with spatial overlap. The technique we employ could be used to greatly increase the dimensionality of entangled photonic systems generated from spontaneous parametric down-conversion, affording greater scalability to optical quantum computing than previously explored.

DOI: 10.1103/PhysRevApplied.16.064048

I. INTRODUCTION

An important process in the field of quantum optics is spontaneous parametric down-conversion (SPDC), a phenomenon wherein excitations within a nonlinear crystal are used to produce correlated photon pairs. SPDC is used to create a pair of entangled photons with zero net polarization. A high-frequency incoming photon (the pump) is converted into a pair of lower-frequency outgoing photons. The photons within a given pair can be entangled in a number of ways: position, momentum, frequency, time, polarization, and orbital angular momentum [1]. To effectively produce more than two entangled photons through SPDC, it is common to employ multiple nonlinear optical elements, which requires tedious optical alignment [1,2].

We present a simple method to generate multiple SPDC rings within the same nonlinear crystal. The versatility of such an approach lends itself to increasing the possible configurations available to create photon pairs with desired correlations in an optics environment (i.e., polarization, wavelength, etc.). We conduct degenerate SPDC utilizing both type I and type II β -barium borate (BBO) crystals. We drive the process with an ultrafast pulsed Ti:sapphire laser, frequency doubled to 404 nm. In the type I case, we use the repeated type I geometry [3]. We use a beam-splitting mask or Gaussian mask (GM) to divide the pump beam into any desired number of “sub-Gaussian” inputs. Each of these sub-Gaussians can in turn generate its own SPDC emission cone. The configuration of the mask will determine the number and the manner of spatial overlap of the down-converted cones, as illustrated in Fig. 1. The pump photons from each sub-Gaussian input have the same optical properties. The intersection of the

SPDC emissions ensures the quantum states of each photon can be made indistinguishable, which can be extended to multipartite states when the rings each contribute more than one photon. The indistinguishability afforded by this overlap is achievable with documented phase compensation techniques, and can allow us to essentially duplicate the quantum state from each SPDC emission at the intersections, yielding excess entangled photons as compared with the single-pump case [4–6].

A similar argument can be followed for the type II interaction where two intersections are already produced [7,8]. Further sources with repeated orthogonal type II crystals have generated an increase of entanglement products [9]. Here, we demonstrate how the input geometry can be altered to accomplish similar and improved results. We show that the orientation of the type II crystal also controls the manner of the cones’ overlap.

II. THEORY

In SPDC, an incident photon is absorbed by a nonlinear medium to excite the emission of a photon pair. These emitted photons can be correlated in a number of ways, with polarization characteristics having been studied extensively [10–13]. For the purpose of this Letter, we only refer to polarization entanglement; arguments, however, can be made for the extension of entanglement across other degrees of freedom between the overlapping SPDC emission cones (i.e., position, energy, momentum, and time). In all cases we present here, the down-conversion is assumed to be degenerate unless it is otherwise explicitly indicated.

It is fruitful to define the Bell states as follows:

$$\begin{aligned} |\phi^\pm\rangle &= \frac{1}{\sqrt{2}} [|HH\rangle \pm e^{i\varphi} |VV\rangle], \\ |\psi^\pm\rangle &= \frac{1}{\sqrt{2}} [|HV\rangle \pm e^{i\varphi} |VH\rangle]. \end{aligned} \quad (1)$$

*Corresponding author. mnngom@umich.edu, ngomm@rpi.edu

[†]These authors contributed equally to this work.

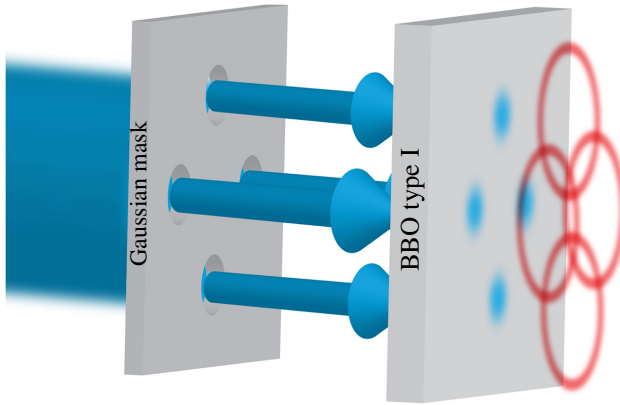


FIG. 1. A four-aperture GM is illustrated. Each “sub-Gaussian” input generates its own SPDC emission cone. The GM design controls the number and the manner of overlap of the down-converted cones.

The ϕ and ψ Bell states are associated with type I and type II processes, respectively, due to their ability to readily prepare photons into the states. The relative phase φ in (1) is determined by the phase acquired during the down-conversion process along with any compensation crystals. Phase compensation techniques are well documented [5,6] and allow $e^{i\varphi}$ in (1) to be set to 1 when $\varphi = \theta_{\text{DC}} + \theta_c = 0$, where the compensation phase (θ_c) exactly cancels out with the relative down-conversion phase (θ_{DC}). When referring to the overall states for a subset of down-converted photons from the intersections of a given mask, we use capitalized Φ and Ψ for the total wave function from types I and II, respectively. This distinction can be represented with the help of operators \mathcal{G} representing the transformation due to the Gaussian mask and \mathcal{D} representing the SPDC event. Both of these operators are set to operate on the Gaussian pump ($|p\rangle$). The operations are described as follows:

$$\begin{aligned} \mathcal{D}(|p\rangle) &= |\phi^\pm\rangle \text{ or } |\psi^\pm\rangle, \\ \mathcal{D}[\mathcal{G}(|p\rangle)] &= |\Phi\rangle \text{ or } |\Psi\rangle. \end{aligned} \quad (2)$$

The system of Bell states is composed of two qubits; thus the usual SPDC process conducted with proper phase compensation could be a source of two entangled qubits. Our approach can also be used to increase the count of indistinguishable photons within the region of overlap.

III. APPARATUS AND EXPERIMENTAL DESIGN

Figure 2 is an illustration of our experimental setup. The laser source (not shown) is a mode-locked regenerative Ti:sapphire laser with repetition rate of 3 kHz, pulse energy of 1.67 mJ, and with a 38-fs pulse duration at 808-nm center wavelength. We use BBO crystals as our nonlinear media for SPDC production. For type I SPDC,

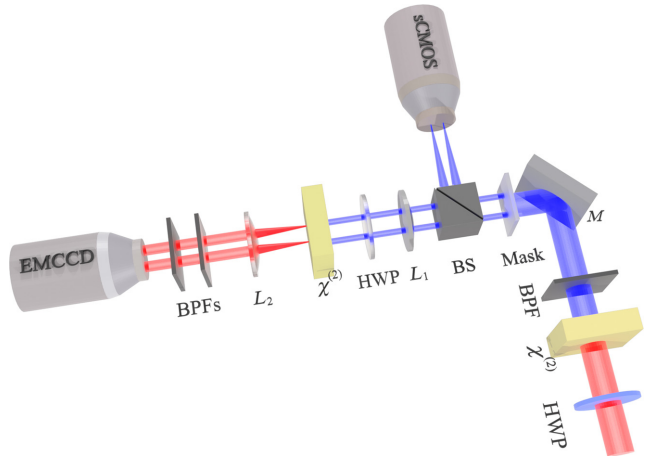


FIG. 2. Schematic of setup including half-wave plates (HWPs), BBOs ($\chi^{(2)}$), band-pass filters (BPFs), beam splitter (BS), mirrors (M), lenses (L), and our beam masks. The SCOMOS and EMCCD image the pump and down-converted light, respectively.

we use two adjacent 500- μm -thick nonlinear crystals that are oriented orthogonally such that a vertically or horizontally polarized pump photon can down-convert into a pair of horizontally or vertically polarized photons in the first (second) crystal. For type II SPDC, we use a single 1000- μm -thick BBO crystal. The crystals are pumped by the frequency-doubled beam (404 nm) via a separate type I BBO crystal as shown in Fig. 2.

The pump beam from the laser system is transformed into sub-Gaussian beams using the GM. The resulting sub-Gaussian beams from each aperture of the GM are then focused by lens L_1 on either the type I or II BBO to produce the desired down-converted cones. The HWP placed after L_1 is used to match the crystals’ polarization axes.

For repeated type I SPDC, we set the polarization of the fundamental beam at 45° , so that the input polarization has equal components along each crystal’s optical axis. For the type II process, we match the fundamental polarization to the crystal optical axis. The down-converted light is collected by lens L_2 and isolated with two BPFs before being captured by an electron-multiplying coupled charged device (EMCCD). An image of the input (pump) beam is recorded with a separate scientific complementary metal oxide semiconductor (SCMOS) camera for each of the masks. The GM is designed to have one, two, three, or four apertures, measuring approximately 2 mm in diameter, and spaced 1.5 mm apart. In the scenario where there are four apertures, the spacing refers to the closest neighbors and not the diagonal of the grid. To ensure that the beam uniformly illuminates the whole structure, we use a 1-cm input beam that is well collimated and filtered such that the intensity distribution is flat along the beam diameter. The GM is also housed in a

kinematic mount that allows us to fine tune its alignment. In both the repeated type I and type II processes, the GM geometry can be seen in the emission pattern from the crystal, revealing an increased brightness in the overlapping regions.

We verify our down-conversion through sufficient filtering before imaging it on the EMCCD. We tune the polarization of the pump beam using the HWP to fully extinguish the observed rings for a single crystal. For the repeated type I crystal, a slight misalignment is introduced to distinguish the SPDC rings, then rotation of the HWP will fully extinguish either ring. To ensure that none of the rings are reflections, we cover the apertures and separately observe the corresponding emission ring disappear. For simultaneous SPDC processes, the overlap of each emission can be adjusted by the mask design. The single-aperture case is given for each process as a reference to the normal SPDC process conducted without a mask.

IV. RESULTS AND DISCUSSION

Illustrations of the expected SPDC emission cones along with the experimental results for repeated type I are displayed in Fig. 3. The increased brightness at the intersection points of the SPDC cone confirms the higher photon density present in these overlapping regions. Figure 3(e) shows the two-aperture GM process conducted with repeated type I. For each aperture, the down-conversion process will create entangled pairs of photons in the $|\phi^+\rangle$ state. We can thus determine one possible form of the wave function for the photons emitted at the overlap

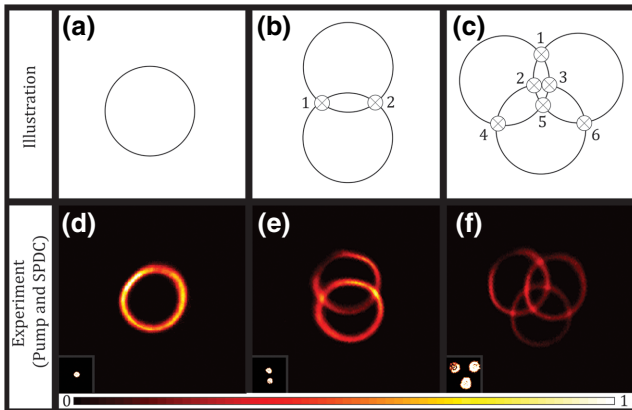


FIG. 3. (a)–(c) Illustrations of repeated type I SPDC cones generated by a single, double, and triple “sub-Gaussian” pump (shown in the inset at bottom left), with the desired overlap labeled. (d)–(f) The corresponding experimental results obtained using GMs designed with one, two, and three apertures. For each case the pump beam is imaged and inset (bottom left) with the SPDC emissions.

as follows:

$$\begin{aligned} |\Phi\rangle = N[& |HHHH\rangle + e^{i\varphi_1} |HHVV\rangle + e^{i\varphi_2} |VVVV\rangle \\ & + e^{i\varphi_3} |VHHH\rangle + e^{i\varphi_4} |HVHV\rangle + e^{i\varphi_5} |HVVH\rangle \\ & + e^{i\varphi_6} |VH VH\rangle + e^{i\varphi_7} |VHHV\rangle], \end{aligned} \quad (3)$$

where $N = 1/\sqrt{8}$ if all outcomes are equally probable and the phases φ_i are determined by the photons’ polarizations and optical path lengths. We use the shorthand $|ij\rangle \otimes |kl\rangle = |ij\rangle |kl\rangle = |ijkl\rangle$ for the outer (tensor) product. The phases can be effectively compensated to obtain a simplified version with the exponential terms set to 1 ($e^{i\varphi} = 1$) [5,6]. The ordering is done to reveal the factoring admitted by the state: rearranging gives us

$$\begin{aligned} |\Phi\rangle = \frac{1}{2\sqrt{2}} [& |HH\rangle (|HH\rangle + |VV\rangle) + |VV\rangle (|VV\rangle + |HH\rangle) \\ & + |HV\rangle (|HV\rangle + |VH\rangle) + |VH\rangle (|VH\rangle + |HV\rangle)] \\ = \frac{1}{\sqrt{2}} [& |\phi^\pm\rangle |\phi^\pm\rangle \pm |\psi^\pm\rangle |\psi^\pm\rangle]. \end{aligned} \quad (4)$$

The addition has been changed to plus or minus in the last line to account for the real values from the exponential phase factors (since compensation can be done differently such that $\varphi = \theta_{DC} + \theta'_c = \pi$). We can now see that the source (repeated type I) behaves differently when it is driven with two pump beams with overlapping emission cones. The resulting state could be an entangled state between products of Bell states, of which now contains the product state $|\psi^\pm\rangle |\psi^\pm\rangle$.

Type II SPDC with the GM is displayed in Figs. 4 and 5. Type II SPDC is inherently less bright than type I due to stricter phase matching conditions, and thus the background noise is more apparent in the captured emissions. The spatial overlap for type II SPDC, shown in Fig. 4(d), already affords polarization entanglement of the emitted photons. Tedious optical alignment must be followed to capture the photons in the region of overlap. However, by applying the GM producing more than a single Gaussian pump, we can completely overlap rings of orthogonal polarization from the separate processes, producing polarization entanglement across the whole overlapped ring, much like in the case of repeated type I, but instead prepared into the $|\psi^+\rangle$ Bell states [14].

The manner of overlap for type II SPDC is controlled first by the spatial separation of each aperture in the GM design. Different GM configurations help determine that a spacing of 2 mm between apertures gives an effective overlap of the SPDC cones, as shown in Fig. 4. The photons in the region of overlap between the SPDC rings could be entangled with each other as distinguishability is erased upon full spatial overlap. Conducting type II SPDC with a

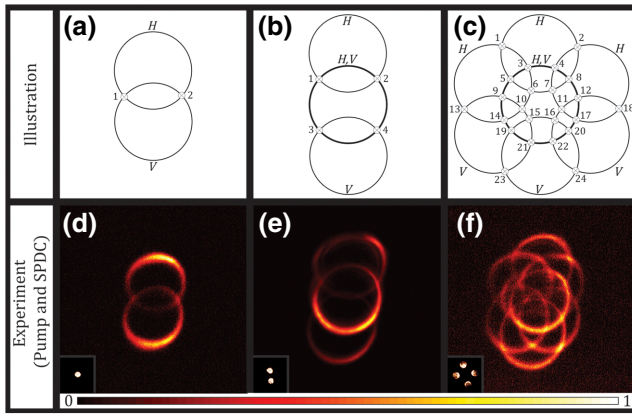


FIG. 4. (a)–(c) Illustrations of Type II SPDC cones generated by a single, double, and quadruple “sub-Gaussian” pump, with the desired overlap labeled. (d)–(f) The corresponding experimental results obtained using GMs designed with one, two, and four apertures. For each case the pump beam is imaged and inset with the SPDC emissions. In (f) the center ring is composed of overlapping rings from the emissions from both the top and bottom apertures.

two-aperture mask is fundamentally different from producing a mixture of type II correlated photons. For example, in Fig. 4(e), we show the two-aperture GM, where the vertical arrangement of the two apertures allows for the two SPDC rings to “share” or have one of their rings to completely overlap. We therefore create a much larger region of overlap. This method makes photon collection far less tedious for type II SPDC. It should be noted that there are many more geometries afforded by conducting the type II process with multiple apertures due to the asymmetry in the emission (with respect to polarization). We only examine one case here, but the process follows similarly for any given emission pattern.

In Fig. 5 we explore four different orientations of the two-aperture GM in type II SPDC emission. We show that by rotating the two-aperture configuration along the azimuthal direction, we can control the region of overlap between the two type II SPDC rings. We can effectively dictate whether the spatial overlap is a whole ring or distinct points of intersection. It is also noticeable

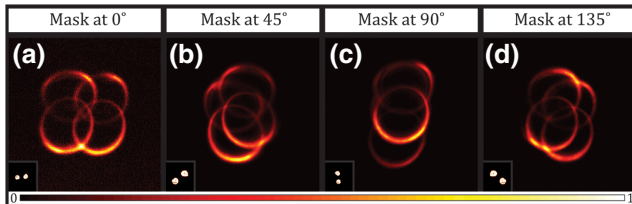


FIG. 5. Type II SPDC emission with a two-aperture mask. (a)–(d) The rotation of the mask demonstrates the full angular control of the emission.

that by superposing (adding) the emission pattern shown in Figs. 5(a) and 5(c), we recover the emission pattern displayed in 4(f).

By symmetry arguments, one can see that the wave function for the photon states at the overlapping regions for the two-aperture GM includes terms that do not appear when computing the outer product of the wave function for a type II process [given in $|\psi^+\rangle$ from Eq. (1)] with itself [14]. The latter gives

$$\begin{aligned} &(|HV\rangle + |VH\rangle) \otimes (|HV\rangle + |VH\rangle) \\ &= |HVHV\rangle + |HVVH\rangle + |VHHV\rangle + |VH VH\rangle, \end{aligned} \quad (5)$$

where we have ignored the normalization and phase factor. However, we can see that the wave function for the overlapping regions should be of the form

$$\begin{aligned} |\Psi\rangle &= N[|HVHV\rangle + |HVVH\rangle + |VHHV\rangle + |VH VH\rangle \\ &\quad + |HHVV\rangle] \\ &= N[2|\psi^\pm\rangle|\psi^\pm\rangle \pm |HHVV\rangle], \end{aligned} \quad (6)$$

where $N = 1/\sqrt{5}$ if all SPDC outcomes are equally probable and the phase terms have been omitted assuming phase compensation has been employed. The last term is determined by the emission polarizations (we have chosen $|HHVV\rangle$ instead of $|VVHH\rangle$). Again the addition has been changed to plus or minus to account for the real values of the phase factor that could be produced with different compensation. The additional term, compare Eq. (5), is due to the fact that the configuration allows the set of intersections (the full ring overlap) in Fig. 4(e) to have the same polarization. Neither of these states is possible in the product of two type II emissions because the sets of intersections belonging to each process must possess one vertically and horizontally polarized photon each.

To increase the amount of correlated photons, care must be taken to compensate for the different phases of the emitted light, ensuring superposition. Accomplishing this leads to an increase in the amount of entangled photon pairs, although it is still dependent on the SPDC configuration and the detection scheme.

V. CONCLUSION

In conclusion, we demonstrate a simple method to increase the number of correlated photon pairs within the region of overlap through SPDC in type I and II BBO crystals. We introduce a Gaussian mask to divide the pump beam into any desired number of “sub-Gaussian” inputs to induce multiple down-converted emission cones from a single nonlinear crystal. We show that the mask

design determines the number and the manner of overlap of the down-converted cones. This method can be easily extended to continuous laser setups, which would eliminate the need to consider clocking effects of the pulse train. This simple approach has promising potential for photonic qubit production setups, being limited only by the size of the nonlinear crystal and pump beam waist (and by extension the pump power and damage threshold of the nonlinear medium per square area). We believe this approach can help simplify and reduce costs for entanglement generation, and thus greatly contribute to photonic based quantum computing. The natural progression of the work will be to quantify the degree of entanglement of the system presented. In quantifying the entanglement of our systems, one might be able to generate an alternative discussion to entanglement monogamy.

-
- [1] G. Jaeger and A. V. Sergienko, Chapter 5- Multi-Photon Quantum Interferometry, *Progress in Optics*, vol. 42. E. Wolf, ed. (Elsevier, 2001), p.277.
 - [2] Z. Zhao, T. Yang, A. Chen, A. N. Zhang, M. Zukowski, and J. W. Pan, Experimental Violation of Local Realism by Four-Photon Greenberger-Horne-Zeilinger Entanglement, *Phys. Rev. Lett.* **91**, 180401 (2003).
 - [3] P. G. Kwiat, E. Waks, A. G. White, I. Appelbaum, and P. H. Eberhard, Ultrabright source of polarization-entangled photons, *Phys. Rev. A* **60**, R773 (1999).
 - [4] No state information is obtained, so this does not conflict with the no-cloning theorem.

- [5] J. B. Altepeter, E. R. Jeffrey, and P. G. Kwiat, Phase-compensated ultra-bright source of entangled photons, *Opt. Express* **13**, 8951 (2005).
- [6] R. Rangarajan, Photonic Sources and Detectors for Quantum Information Protocols: A Trilogy in Eight Parts, p. 15–55, Thesis Dissertation, University of Illinois Urbana-Champaign, (2010).
- [7] P. G. Kwiat, K. Mattle, H. Weinfurter, A. Zeilinger, A. V. Sergienko, and Y. Shih, New High-Intensity Source of Polarization-Entangled Photon Pairs, *Phys. Rev. Lett.* **75**, 4337 (1995).
- [8] A. Zeilinger, M. A. Horne, H. Weinfurter, and M. Zukowski, Three Particle Entanglements from two Entangled Pairs, *Phys. Rev. Lett.* **78**, 3031 (1997).
- [9] M. L. Fanto, R. K. Erdmann, P. M. Alsing, C. J. Peters, and E. J. Galvez, in *Quantum Information and Computation IX*, vol. 8057 E. Donkor, A. R. Pirich, and H. E. Brandt, eds., International Society for Optics and Photonics, (SPIE, 2011), p. 41.
- [10] C. K. Hong and L. Mandel, Theory of parametric frequency down conversion of light, *Phys. Rev. A* **31**, 2409 (1985).
- [11] M. H. Rubin, D. N. Klyshko, Y. H. Shih, and A. V. Sergienko, Theory of two-photon entanglement in type II optical parametric down-conversion, *Phys. Rev. A* **50**, 5122 (1994).
- [12] T. E. Keller and M. H. Rubin, Theory of two-photon entanglement for spontaneous parametric down-conversion driven by a narrow pump pulse, *Phys. Rev. A* **56**, 1534 (1997).
- [13] S. Franke-Arnold, S. M. Barnett, M. J. Padgett, and L. Allen, Two-photon entanglement of orbital angular momentum states, *Phys. Rev. A* **65**, 033823 (2002).
- [14] Compensating to set the exponential phase factor to +1.